Effect of Baffles on the N_2-seeded Snowflake Minus Low-Field Side Configuration in the Tokamak à Configuration Variable (TCV)

S. Gorno[1], O. Février[1], H. Reimerdes[1], C. Theiler[1], A. Thornton[2], C. Colandrea[1], H. De Oliveira[1], B. P. Duval[1], H. Raj[1], the TCV team[a], and the Eurofusion MST1 team[b].

[1] *Ecole Polytechnique Fédérale de Lausanne (EPFL), Swiss Plasma Center (SPC), CH-1015 Lausanne, Switzerland*

[2] *CCFE, Culham Science Centre, Abingdon, Oxon, OX14 3DB, UK*

[a] *See the author list of S. Coda et al. 2019 Nucl. Fusion 59 112023*

[b] *See author list of B. Labit et al 2019 Nucl. Fusion 59 086020*

Introduction Plasma exhaust remains a major challenge in magnetic confinement fusion, as an unmitigated heat flux reaching the wall in future reactors is predicted to greatly exceed material limits. Alternative divertor configurations are being developed on current devices, should the current exhaust solution, featuring a single null (SN) configuration, not scale to reactors such as DEMO. One such configuration is the Snowflake minus Low-Field Side (SF-LFS) [1, 2] that features a secondary X-point in the common flux region. This increases the number of strike-points and creates an enlarged region of low poloidal field, which is expected to give rise to greater radiative losses and lower target temperatures [3]. In TCV, the SF-LFS exhibits reduced peak outer target heat fluxes with respect to the SN configuration, as measured by Langmuir probes (LPs) [4] and the infra-red thermography system [5].

The effect of N_2 seeding has been explored in TCV for the SN, achieving detachment with target heat flux reductions of up to 90% [6]. Furthermore, it is seen that scrape-off layer power radiation increases and a stable X-point radiator forms, as observed also in ASDEX-upgrade [7]. However, N_2 seeding can lead to core penetration at low densities [6], diluting the plasma core. In the SF-LFS in TCV, N_2 seeding can result in a radiation zone between the two X-points [8]: does this offer a route to better divertor-core compatibility?

Discussion TCV has installed gas baffles to increase divertor closure, leading to a higher divertor neutral pressure and a reduced core density detachment threshold for a given SN configuration [9, 10]. A large flux expansion in the SF's inter-null region makes this geometry difficult to baffle without large fluxes impinging upon the outer baffle, as recorded in the 2019 TCV baffle campaign. A more 'baffle-compatible' SF-LFS geometry (ohmic, L-mode, I_p=250 kA, core density of $< n_e >= 4.5 \times 10^{19} \mathrm{m}^{-3}$) was thus developed for the 2021 baffle campaign (Fig. 1). LP target ion saturation current, J_{sat}, profiles demonstrate a reduced baffle interaction and improvement in target coverage in the 'baffle-compatible' case. The SF-LFS divertor neutral pressure increases with baffles (Fig. 2), similarly to that for the baffled SN [9].

This increase in divertor neutral pressure leads to a reduction in target T_e at both active outer strike-points (SP2, SP4) of the SF-LFS (Fig. 3). Here, the peak ion flux is only slightly reduced, but the total ion flux is largely unaffected. The peak and total heat flux are, however, reduced by over a third with respect to unbaffled configurations, with equal relative reductions at both outer strike-points (SP2, SP4). The power sharing relation between SP2 and SP4, controlled by the SF X-point separation, is clearly not affected by the presence of baffles. Therefore, the 'optimal' X-point separation, where the total or peak heat flux is equal at each active outer strike-point, remains similar with and without baffles.

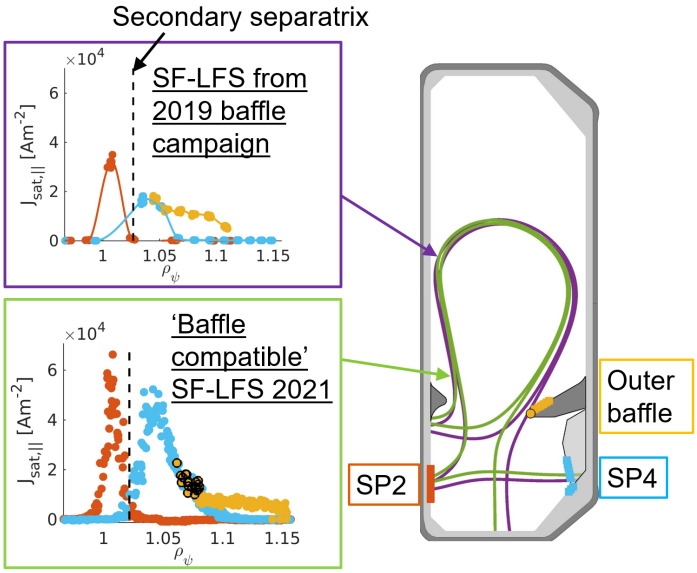

Figure 1: *Right: Equilibrium reconstruction of SF-LFS separatrices in the TCV vessel from the 2019 (purple) and 2021 (green) baffle campaigns. Wall-embedded LPs are plotted at SP2, SP4 and the LFS baffle. Left: LP J_{sat} profiles, where points with black outline represent the new baffle tip LP, installed for the 2021 campaign.*

A close-to-optimal SF-LFS (in terms of peak heat flux) is now compared with a SN configuration of similar density. Target T_e profiles of the outer SF divertor closely match that of the SN (Fig 4). Ion and heat flux profiles highlight an advantage for the SF; the outer flux is directed to two strike-points, thereby reducing the power load and peak heat flux. However, at the inner target, this SF-LFS sees an 83% increase in peak heat flux with respect to the SN, largely due to an increase in peak target T_e. Further analysis will investigate whether the outer target heat flux reduction is due to increased radiation levels and/or simply redistribution to the inner target.

With N_2 seeding, we see a reduction in outer target ion flux, power load and electron temperature in the SF-LFS, as for the SN, with and without baffles. The outer strike-points of the SF-LFS are compared with the outer strike-point of the SN by combining SP2 and SP4 as follows. The total fluxes are taken as the sum of the flux integrated over each outer target; the peak quantities are taken as the maximum over the two strike-point regions. The presence of baffles does not affect the total target ion flux, but reduces the peak target temperature and

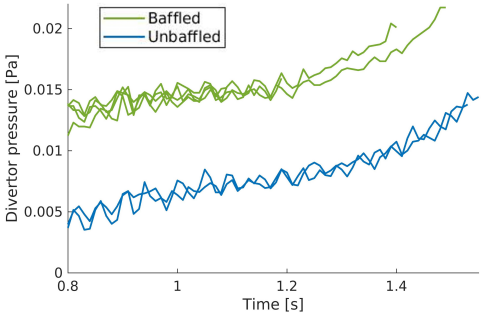

Figure 2: *Divertor neutral pressure measured in the common flux region of the baffle-compatible SF-LFS geometry.*

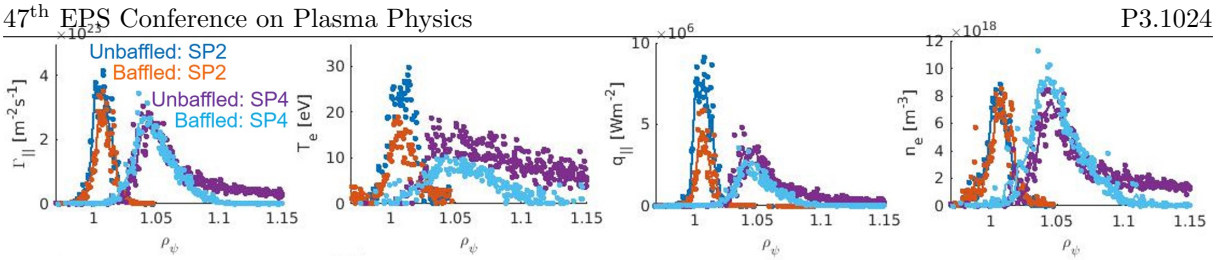

Figure 3: *Outer target LP profiles for baffled and unbaffled SF-LFS: parallel ion flux, $\Gamma_{||}$; electron temperature, T_e; parallel heat flux, $q_{||}$; sheath edge electron density, n_e.*

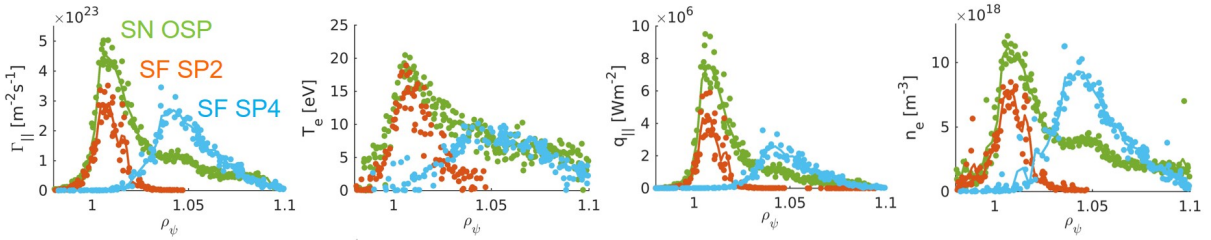

Figure 4: *Outer LP target profiles of baffled SF-LFS (SP2 and SP4) and SN (outer strike-point).*

hence the heat flux, throughout the N_2 seeding ramp (Fig 5). When comparing the SF-LFS with the SN configuration, we see that the peak target temperature is unchanged, but that the SF exhibits a lower total target ion flux. This once again leads to a decrease in the total target heat flux, proving the SF-LFS to be advantaged by its ability to reduce outer target power loads with respect to the SN.

The effect of baffles and the SF geometry on core compatibility is evaluated using an estimate of the average charge of core plasma ions, Z_{eff}, and the energy confinement time, τ_{exp}. The former can be expressed as $Z_{eff} = (\Sigma_i Z_i^2 n_i)/n_e$, and is used to indicate the level of core impurity pollution. It may be estimated from the plasma loop voltage and the profile-averaged core T_e from Thomson Scattering (TS), assuming steady state conditions and neoclassical conductivity [11, 12, 13, 14]. This Z_{eff} increases with N_2 injection, indicating core N_2 penetration (Fig 6(a)). The SF-LFS generally has a stronger increase in Z_{eff} than the SN configuration with N_2 seeding, indicating stronger core impurity penetration.

The energy confinement time is defined as the ratio of stored energy to the total input power: $\tau_{exp} = W_{MHD}/P_{in}$, where $W_{MHD} = 3\pi \iint (2n_e T_e) r dr dz$, assuming $n_e = n_i$, $T_e = T_i$, where again

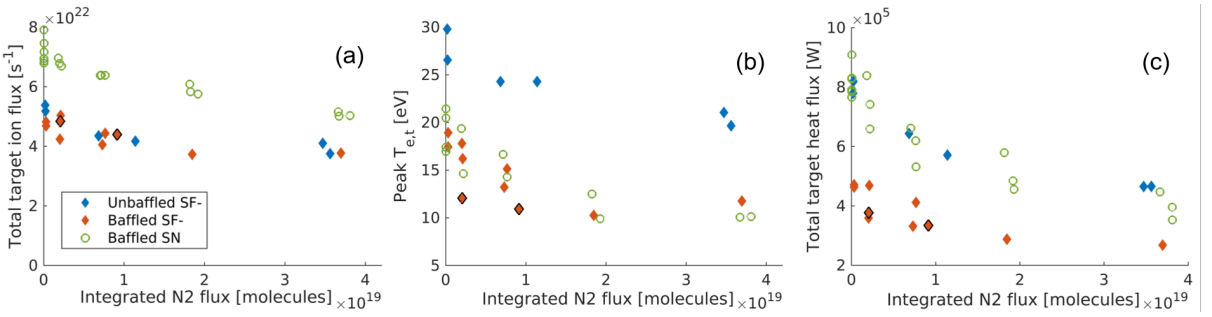

Figure 5: *Outer target quantities as a function of time-integrated N_2 flux for unbaffled SF-LFS, baffled SF-LFS and baffled SN. (a) Target-integrated ion flux; (b) peak target T_e; (c) target-integrated heat flux.*

the temperature and density profiles are obtained from the TS system. Fig 6(b) shows that the energy confinement time degrades with N_2 injection. A slight decrease in core confinement is seen for the SF-LFS in comparison to the SN, likely due to the increase in core N_2 penetration deduced from Z_{eff}.

Conclusion The SF-LFS can be efficiently baffled to increase the divertor neutral pressure, similarly to the baffled SN configuration. Baffle-compatible geometries have been developed to decrease baffle-plasma interaction, whilst maintaining the ability to obtain SF-LFS configurations of various X-point separations. Baffles effectively reduce the target temperature and heat flux, and have little effect on the power sharing between the outer strike-points of the SF-LFS. When comparing the outer divertor of a close-to-'optimal' baffled SF-LFS with the SN configuration, we see no difference in peak target temperature, but at least a 25% reduction in total target ion flux throughout the N_2 seeding ramp, resulting in an overall reduction in target heat flux. This advantage of the SF-LFS over the SN comes, however, at the cost of a slightly stronger core N_2 penetration and concomitant degradation in core energy confinement.

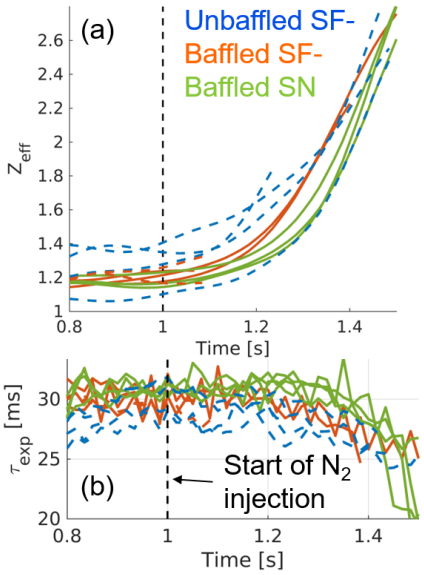

Figure 6: *(a) Z_{eff}, (b) τ_{exp}; for unbaffled and baffled SF-LFS, and baffled SN. N_2 seeding ramp begins at 1s for all cases, reaching a time-integrated flux of 4.9×10^{19} molecules by 1.4s.*

Acknowledgements This work has been carried out within the framework of the EUROfusion Consortium and has received funding from the Euratom research and training programme 2014-2018 and 2019-2020 under grant agreement number 633053. The views and opinions expressed herein do not necessarily reflect those of the European Commission. This work was supported in part by the Swiss National Science Foundation.

References

[1] D. Ryutov *et al.*, Physics of Plasma **14**, 064502 (2007)
[2] D. Ryutov and V. Soukhanovskii, Physics of Plasma **22**, 110901 (2015)
[3] H. Reimerdes *et al.*, Plasma Physics and Controlled Fusion **55**, 12 (2013)
[4] B. Labit *et al.*, Nuclear Materials and Energy **12**, 1015-1019 (2017)
[5] R. Maurizio *et al.*, Nuclear Fusion **59**, 016014 (2019)
[6] O. Février *et al.*, Plasma Physics and Controlled Fusion **62**, 035017 (2020)
[7] M. Bernert *et al.*, Nuclear Materials and Energy **12**, 111-118 (2017)
[8] H. Reimerdes *et al.*, Nuclear Fusion **57**, 126007 (2017)
[9] O. Février *et al.*, Nuclear Materials and Energy **27**, 100977 (2021)
[10] H. Reimerdes *et al.*, Nuclear Fusion **61**, 2 (2021)
[11] O. Sauter *et al.*, Physics of Plasmas **8**, 2199 (2001)
[12] O. Sauter, C. Angioni and Y. R. Lin-Liu, Physics of Plasmas **6**, 2834 (1999)
[13] O. Sauter, C. Angioni and Y. R. Lin-Liu, Physics of Plasmas **9**, 5140 (2002)
[14] Y. R. Lin-Liu and R. L. Miller, Physics of Plasmas **2**, 5 (1995)